TECHNISCHE MECHANIK, Band 19, Heft 4, (1999), 259-268
Manuskripteingang: 03. Mai 1999

Determination of the Elasticity Tensor of Non-Orthotropic Cellular Sandwich Cores

J. Hohe, W. Becker

Aim of the present study is the determination of the components of the effective elasticity tensor of general twodimensional cellular materials such as cellular cores used in structural sandwich panels. The homogenization of the microstructure is performed by means of a strain energy based concept considering a representative volume element. The strain energy is evaluated by an analytical approach based on Timoshenko's beam theory and comparativly in a pure numerical approach using the finite element method. Both approaches agree well in the exemplary analysis of a non-orthotropic triangular sandwich core.

1 Introduction

Structural sandwich panels are widespread in lightweight construction since the principle of sandwich construction enables high bending stiffness values at very low weight. A typical sandwich panel consists of three layers: The upper and the lower face sheet made of a homogeneous material which are separated by a low-density core (see Figure 1). The core acts as a stabilizer for the face sheets and carries the transverse shear loads. Typically, the core is made of a twodimensional cellular material.

For reasons of numerical efficiency, the analysis of cellular materials is performed in terms of effective properties rather than by an analysis considering the real microstructure. Thus, the microstructure has to be homogenized. Numerous studies regarding the effective properties of cellular sandwich cores have been performed, since the pioneering work of Kelsey et al. (1958) and Chang and Ebcioglu (1961) has been published (see e.g. Gibson and Ashby, 1988; Noor et al., 1996 or Torquato et al., 1998). Most of these studies are concerned with one special geometry of the cellular core material and many are restricted to the transverse elastic properties. Only few studies are concerned with the non-orthotropic case (e.g. Overaker et al., 1998) who consider non-orthotropic hexagonal cells . To the authors' knowledge, no comprehensive analysis is available for the case of a non-orthotropic cellular material with general cell topology and geometry.

The homogenization of the given microstructure can be performed in several ways. Most studies in literature simply redistribute stresses and strains in order to obtain the effective properties. On the other hand, rigorous mathematical theories as the variational approach by Hashin and Shtrikman (1962) or the perturbation theory based approach by Sanchez-Palencia (1980) are available. The present study uses a strain energy based approach. In this context, the mechanical behaviour of a representative volume element made of the given microstructure and a corresponding volume element made of the homogeneous "effective" medium is considered to be equal on the macroscopic level if an equivalent deformation causes

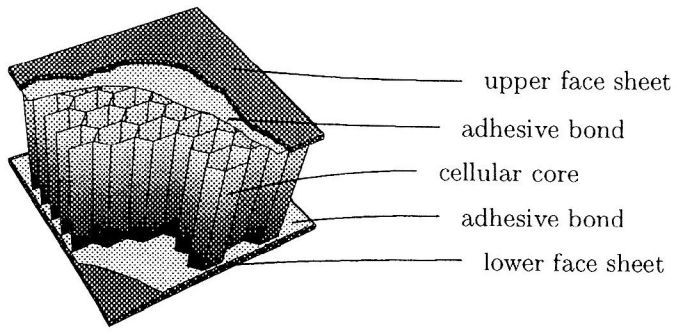

Figure 1: Principle of Structural Sandwich Panels

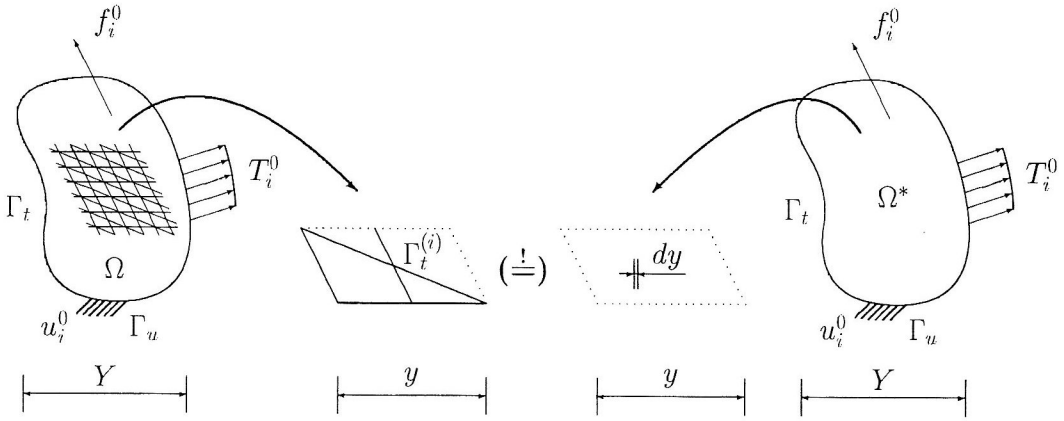

Figure 2: Concept of the Representative Volume Element

equal strain energy for both volume elements. In two preceeding papers, this method was successfully applied to triangular cell structures (Hohe and Becker, 1999) as well as quadrilateral and hexagonal cell structures (Hohe et al., 1999). In the present paper, the method is applied to twodimensional cellular media with general cell geometry.

2 Concept of Energetic Homogenization

Consider a mechanical body Ω made of a cellular material. The body is bounded by an external boundary Γ on which some external stresses T_i^0 and prescribed displacements u_i^0 are applied (see Figure 2). This body is to be replaced by a body Ω^* with the same external shape subject to the same external boundary conditions made of a homogeneous medium with yet unknown properties.

Since the material properties do not depend on the external shape and loading conditions of the entire body Ω or Ω^*, a representative volume element of Ω and a corresponding volume element of Ω^* can be considered. The material properties of the effective material have to be chosen in such a way that the mechanical behaviour of both volume elements is equal on the macroscopic level. Within the framework of the present study, equivalence of both volume elements is assumed, if the strain energy stored in both volume elements is equal for macroscopically equivalent strain states. Therefore, the condition

$$\int_{\Omega} w(\varepsilon_{ij})\,\mathrm{d}V = \int_{\Omega^*} w^*(\varepsilon_{ij}^*)\,\mathrm{d}V^* \tag{1}$$

has to be satisfied, where w and ε_{ij} denote strain energy and strain tensor, respectively and quantities marked $(\ldots)^*$ are quantities with respect to the effective medium. According to Bishop and Hill (1951), equivalence of the strain states on the macroscopic level is assumed if

$$\int_{\Omega} \varepsilon_{ij}\,\mathrm{d}V = \int_{\Omega^*} \varepsilon_{ij}^*\,\mathrm{d}V^* \tag{2}$$

holds. Thus, for determination of the effective properties, both volume elements have to be deformed by a number of independent characteristic strain states ε_{ij} and ε_{ij}^* which satisfy equation (2). Homogeneous effective strain states $\varepsilon_{ij} = \bar{\varepsilon}_{ij}$ can be used without any loss in generality. Next, the strain energy is computed for both volume elements and the effective properties are determined in such a way that equation (1) is satisfied. In this context, the strain energy can be evaluated either analytically or numerically.

3 Analytical Approach

The first approach for the determination of the strain energy in the representative volume element to be described is a simplified analytical one. An appropriate representative volume element for general

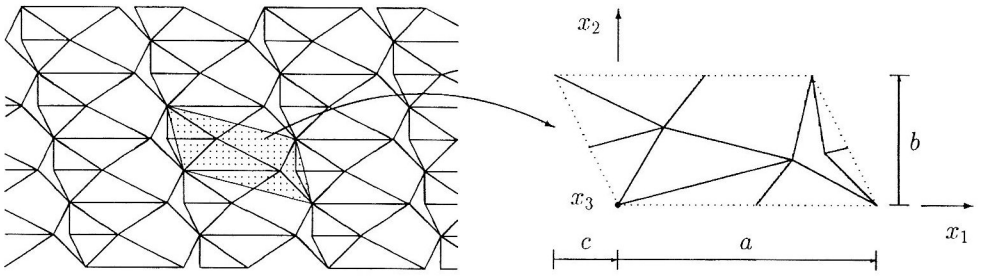

Figure 3: Representative Volume Element for General Twodimensional Cellular Materials

twodimensional periodic cellular materials is presented in Figure 3. Independent of the cell topology and geometry, a parallelogram-shaped representative volume element as in Figure 3 can always be found. With no loss in generality, a local coordinate system x_i can be introduced.

Next, the cellular structure in the representative volume element is splitted up into individual cell wall elements according to Figure 4. The total strain energy in the entire volume element then is given by the sum of the strain energies in all individual cell wall elements. The mechanical behaviour of all individual cell wall elements can be expressed in terms of the deflections (displacements in three directions and rotation with respect to the transverse (x_3-) axis) of the cell wall ends (subsequently termed nodal points).

In order to compute the strain energy of an individual cell wall element, a local coordinate system $\tilde{x}_i$ according to Figure 5 is introduced. The displacement and deformation field is assumed to consist of three parts:

- normal deformation in the $\tilde{x}_1$-$\tilde{x}_3$-plane

$$\begin{aligned} \tilde{u}_1^I(\tilde{x}_i) &= \tilde{v}_{(1)1} + \frac{\tilde{x}_1}{l}\left(\tilde{v}_{(2)1} - \tilde{v}_{(1)1}\right) \\ \tilde{u}_2^I(\tilde{x}_i) &= -\frac{\nu}{1-\nu}\left(\frac{1}{l}\left(\tilde{v}_{(2)1} - \tilde{v}_{(1)1}\right) + \bar{\varepsilon}_{33}\right)\tilde{x}_2 \\ \tilde{u}_3^I(\tilde{x}_i) &= \bar{\varepsilon}_{33}\tilde{x}_3 \end{aligned} \tag{3}$$

- bending and shear deformation according to Timoshenko beam theory in the $\tilde{x}_1$-$\tilde{x}_2$-plane

$$\begin{aligned} \tilde{u}_1^{II}(\tilde{x}_i) &= -\left(\frac{1}{EI}\left(\frac{1}{2}C_1\tilde{x}_1^2 + C_2\tilde{x}_1 + C_3\right) + \frac{2(1+\nu)}{EA_s}C_1\right)\tilde{x}_2 \\ \tilde{u}_2^{II}(\tilde{x}_i) &= \frac{1}{EI}\left(\frac{1}{6}C_1\tilde{x}_1^3 + \frac{1}{2}C_2\tilde{x}_1^2 + C_3\tilde{x}_1 + C_4\right) \\ \tilde{u}_3^{II}(\tilde{x}_i) &= 0 \end{aligned} \tag{4}$$

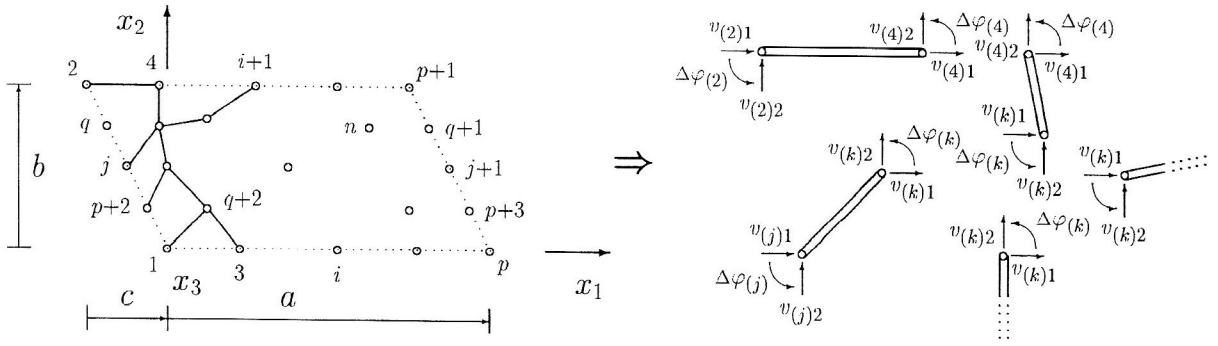

Figure 4: Decomposition of the Representative Volume Element into Individual Cell Wall Elements

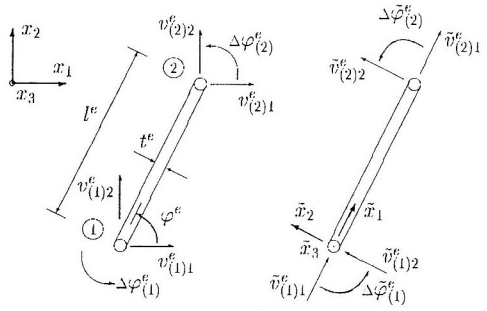

Figure 5: Cell Wall Element

- transverse shear deformation ($\tilde{x}_1$-$\tilde{x}_3$-plane)

$$\begin{aligned} \tilde{u}_1^{III}(\tilde{x}_i) &= 0 \\ \tilde{u}_2^{III}(\tilde{x}_i) &= 0 \\ \tilde{u}_3^{III}(\tilde{x}_i) &= \tilde{v}_{(1)3} + \frac{\tilde{x}_1}{l}\left(\tilde{v}_{(2)3} - \tilde{v}_{(1)3}\right) \end{aligned} \tag{5}$$

where l, h and t denote length, height and thickness of the considered cell wall element, respectively, while E and ν are the elastic constants of the cell wall material, $I = ht^3/12$ and $A_s = 5/6ht$. C_1 to C_4 are constants which have to be determined from the boundary conditions according to standard beam theory at the cell wall ends. The variable $\tilde{v}_{(i)j}$ denotes the displacement at nodal point i in direction $\tilde{x}_j$ while $\Delta\varphi_{(i)}$ is the rotation at nodal point i with respect to the $\tilde{x}_3$-axis (see Figure 5).

The total displacement field $\tilde{u}_i$ is given by the sum of the three parts given in equations (3) to (5). The strain field of the cell wall element is derived from $\tilde{u}_i$ by differentiation with respect to $\tilde{x}_j$. Subsequently, the stress field is obtained by inserting the strain field into Hooke's law and the strain energy density is derived as the sum of the products of the components of stress and strain. Finally, the total strain energy of the cell wall element is obtained by integration of the strain energy density with respect to the volume of the cell wall element. This lengthy but straightforward calculation results in:

$$\begin{aligned} W = \frac{E}{2(1-\nu^2)} htl \Bigg(& \begin{pmatrix} \frac{\tilde{v}_{(1)1}}{l} \\ \frac{\tilde{v}_{(2)1}}{l} \\ \bar{\varepsilon}_{33} \end{pmatrix}^T \begin{pmatrix} 1 & -1 & -\nu \\ -1 & 1 & \nu \\ -\nu & \nu & 1 \end{pmatrix} \begin{pmatrix} \frac{\tilde{v}_{(1)1}}{l} \\ \frac{\tilde{v}_{(2)1}}{l} \\ \bar{\varepsilon}_{33} \end{pmatrix} \\ & + \beta \begin{pmatrix} \frac{\tilde{v}_{(1)2}}{l} \\ \Delta\tilde{\varphi}_{(1)} \\ \frac{\tilde{v}_{(2)2}}{l} \\ \Delta\tilde{\varphi}_{(2)} \end{pmatrix}^T \begin{pmatrix} 1 & \frac{1}{2} & -1 & \frac{1}{2} \\ \frac{1}{2} & \frac{1}{4} & -\frac{1}{2} & \frac{1}{4} \\ -1 & -\frac{1}{2} & 1 & -\frac{1}{2} \\ \frac{1}{2} & \frac{1}{4} & -\frac{1}{2} & \frac{1}{4} \end{pmatrix} \begin{pmatrix} \frac{\tilde{v}_{(1)2}}{l} \\ \Delta\tilde{\varphi}_{(1)} \\ \frac{\tilde{v}_{(2)2}}{l} \\ \Delta\tilde{\varphi}_{(2)} \end{pmatrix} \\ & + \frac{1}{12}\frac{t^2}{l^2} \begin{pmatrix} \Delta\tilde{\varphi}_{(1)} \\ \Delta\tilde{\varphi}_{(2)} \end{pmatrix}^T \begin{pmatrix} 1 & -1 \\ -1 & 1 \end{pmatrix} \begin{pmatrix} \Delta\tilde{\varphi}_{(1)} \\ \Delta\tilde{\varphi}_{(2)} \end{pmatrix} \\ & + \frac{1-\nu}{2} \begin{pmatrix} \frac{\tilde{v}_{(1)3}}{l} \\ \frac{\tilde{v}_{(2)3}}{l} \end{pmatrix}^T \begin{pmatrix} 1 & -1 \\ -1 & 1 \end{pmatrix} \begin{pmatrix} \frac{\tilde{v}_{(1)3}}{l} \\ \frac{\tilde{v}_{(2)3}}{l} \end{pmatrix} \Bigg) \end{aligned} \tag{6}$$

$$\beta = \frac{1}{(1+\alpha)^2}\left(\frac{t^2}{l^2} + \frac{1}{2}\alpha^2(1-\nu)\right)$$

$$\alpha = \begin{cases} \frac{12}{5}(1-\nu)\frac{t^2}{l^2} & \text{Timoshenko-theory} \\ 0 & \text{Euler-Bernoulli-theory} \end{cases}$$

The remaining task consists of the determination of the nodal deflections $v_{(i)j}$ and $\Delta\varphi_{(i)}$ for the entire volume element. A complete linear system of $4n$ equations for the $4n$ unknown deflections can be derived by the following considerations:

- No rigid body motions of the representative volume element are permitted. Therefore (e.g.):

$$\begin{aligned} v_{(1)1} &= 0 \\ v_{(1)2} &= 0 \\ v_{(1)3} &= 0 \\ v_{(p)2} &= 0 \end{aligned} \tag{7}$$

- Since homogeneous effective strain states are considered on the effective level, periodic boundary conditions have to be stated with respect to the boundaries of the representative volume element. In this case, the same relative displacement field is obtained in all volume elements which set up the entire structure. To ensure that neighbouring volume elements fit at their joint boundaries during deformation, the following periodicity conditions apply:

$$\begin{aligned} \Delta\varphi_{(i)} &= \Delta\varphi_{(i+1)} && , \quad i = 1,3,\ldots,p \\ v_{(p)l} - v_{(i)l} &= v_{(p+1)l} - v_{(i+1)l} && , \quad i = 1,3,\ldots,(p-2) \quad , \quad l = 1,2,3 \\ \Delta\varphi_{(j)} &= \Delta\varphi_{(j+1)} && , \quad j = (p+2),(p+4),\ldots,q \\ v_{(2)l} - v_{(j)l} &= v_{(p+1)l} - v_{(j+1)l} && , \quad j = (p+2),(p+4),\ldots,q \quad , \quad l = 1,2,3 \\ \Delta\varphi_{(1)} &= \Delta\varphi_{(p)} \end{aligned} \tag{8}$$

- The macroscopic strain field $\bar{\varepsilon}_{ij}$ has to be related to the nodal deflections. Therefore, the volume integral in equation (2) is rewritten into a surface integral by means of Green's theorem:

$$\bar{\varepsilon}_{ij} = \frac{1}{2}\frac{1}{V}\int_{\Gamma} (u_i n_j + u_j n_i)\ \mathrm{d}S \tag{9}$$

where n_i are the components of the outward normal vector on Γ. The integration in equation (9) can be performed, if the displacement field along the boundaries of the representative volume element between nodal points is interpolated. Using the mid-surface displacement of a cell wall element according to equations (3) to (5) as an interpolation function and considering the periodicity conditions (8), the following equations are obtained:

$$\begin{aligned} \bar{\varepsilon}_{11} &= \frac{v_{(p)1} - v_{(1)1}}{a} \\ \bar{\varepsilon}_{22} &= \frac{v_{(2)2} - v_{(1)2}}{b} + \frac{c}{a}\frac{v_{(p)2} - v_{(1)2}}{b} \\ \bar{\varepsilon}_{23} &= \frac{1}{2}\left(\frac{v_{(2)3} - v_{(1)3}}{b} + \frac{c}{a}\frac{v_{(p)3} - v_{(1)3}}{b}\right) \\ \bar{\varepsilon}_{13} &= \frac{1}{2}\frac{v_{(p)3} - v_{(1)3}}{a} \\ \bar{\varepsilon}_{12} &= \frac{1}{2}\left(\frac{v_{(p)2} - v_{(1)2}}{a} + \frac{v_{(2)1} - v_{(1)1}}{b} + \frac{c}{a}\frac{v_{(p)1} - v_{(1)1}}{b}\right) \end{aligned} \tag{10}$$

- Since no external forces are acting, the stress resultants at the internal nodal points have to be in equilibrium. In addition, the sum of the stress resultants of corresponding points on the surfaces of the representative volume element have to vanish to ensure periodicity of the stress field:

$$\begin{aligned} F_{(1)l} + F_{(2)l} + F_{(p)l} + F_{(p+1)l} &= 0 \\ M_{(1)} + M_{(2)} + M_{(p)} + M_{(p+1)} &= 0 \\ \left.\begin{aligned} F_{(i)l} + F_{(i+1)l} &= 0 \\ M_{(i)} + M_{(i+1)} &= 0 \end{aligned}\right\} &, \quad \begin{cases} i = 3,5,\ldots,(p-2) \\ i = (p+2),(p+4),\ldots,q \end{cases} \\ \left.\begin{aligned} F_{(k)l} &= 0 \\ M_{(k)} &= 0 \end{aligned}\right\} &, \quad k = (q+2),(q+3),\ldots n \\ & \qquad\qquad l = 1,2,3 \end{aligned} \tag{11}$$

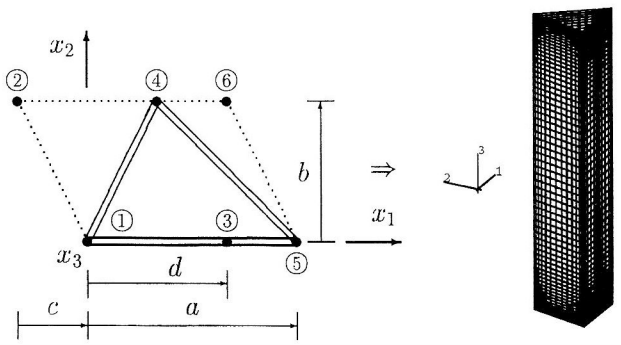

Figure 6: Numerical Approach (Triangular Core Geometry)

The stress resultants at the ends of the individual cell wall elements are easily obtained by differentiation of equation (6) with respect to the nodal deflections. Since the assumption for the displacement field for the individual cell wall elements satisfies the local equilibrium, the global equilibrium with respect to the forces on the entire volume element is satisfied identically. Therefore, three equations of (11) have to be omitted.

The system of equations (7), (8), (10) and (11) is solved by Gaussian elimination.

4 Numerical Approach

Alternatively to the analytical approach, the strain energy can be computed by a pure numerical analysis using the finite element method. For this purpose, the cell walls are meshed by four-node shell elements (see Figure 6, where a general triangular cell geometry is used as an example). A shear flexible shell theory in an enhanced strain formulation is adopted which uses six degrees of freedom per node. The finite element model is deformed by prescribed displacements of the top and bottom plane ($x_3 = \pm h/2$) according to

$$u_i^0 = \begin{pmatrix} x_1\bar{\varepsilon}_{11} & + 2x_2\bar{\varepsilon}_{12} & + 2x_3\bar{\varepsilon}_{13} \\ & x_2\bar{\varepsilon}_{22} & + 2x_3\bar{\varepsilon}_{23} \\ & & x_3\bar{\varepsilon}_{33} \end{pmatrix} \tag{12}$$

which is the displacement field that would occur on these planes if the representative volume element were made of a homogeneous material. Periodic boundary conditions are applied to all remaining surfaces of the representative volume element:

$$\left.\begin{array}{rcl} v_{(1)l}(x_3) - v_{(p)l}(x_3) & = & v_{(1)l}(\frac{h}{2}) - v_{(p)l}(\frac{h}{2}) \\ \Delta\varphi_{(1)l}(x_3) - \Delta\varphi_{(p)l}(x_3) & = & 0 \\ v_{(i)l}(x_3) - v_{(i+1)l}(x_3) & = & v_{(i)l}(\frac{h}{2}) - v_{(i+1)l}(\frac{h}{2}) \\ \Delta\varphi_{(i)l}(x_3) - \Delta\varphi_{(i+1)l}(x_3) & = & 0 \end{array}\right\} \quad i = 1,3,\ldots,q \ , \quad l = 1,2,3 \tag{13}$$

where $v_{(i)l}(x_3)$ denotes the displacement of a finite element node on line i at x_3 with respect to direction x_l while $\Delta\varphi_{(i)l}(x_3)$ denotes the rotation of a finite element node on line i at x_3 with respect to the x_l-axis.

5 Example

The analysis is performed by both the analytical and the numerical approach using a general non-orthotropic triangular sandwich core according to Figure 6 as an example. A constant value of $d/a = 0.5$ is adopted while c/a is varied from $-3/2$ to $3/2$ and five different values of b/a are considered. A constant relative density of $\bar{\rho} = 0.2$ is assumed during all parameter studies by an appropriate choice of the cell wall thickness t^e (which is assumed equal for all cell walls). The computed components of the effective elasticity tensor are presented in Figures 7 and 8. Here, lines denote analytical results while finite element results are marked by symbols.

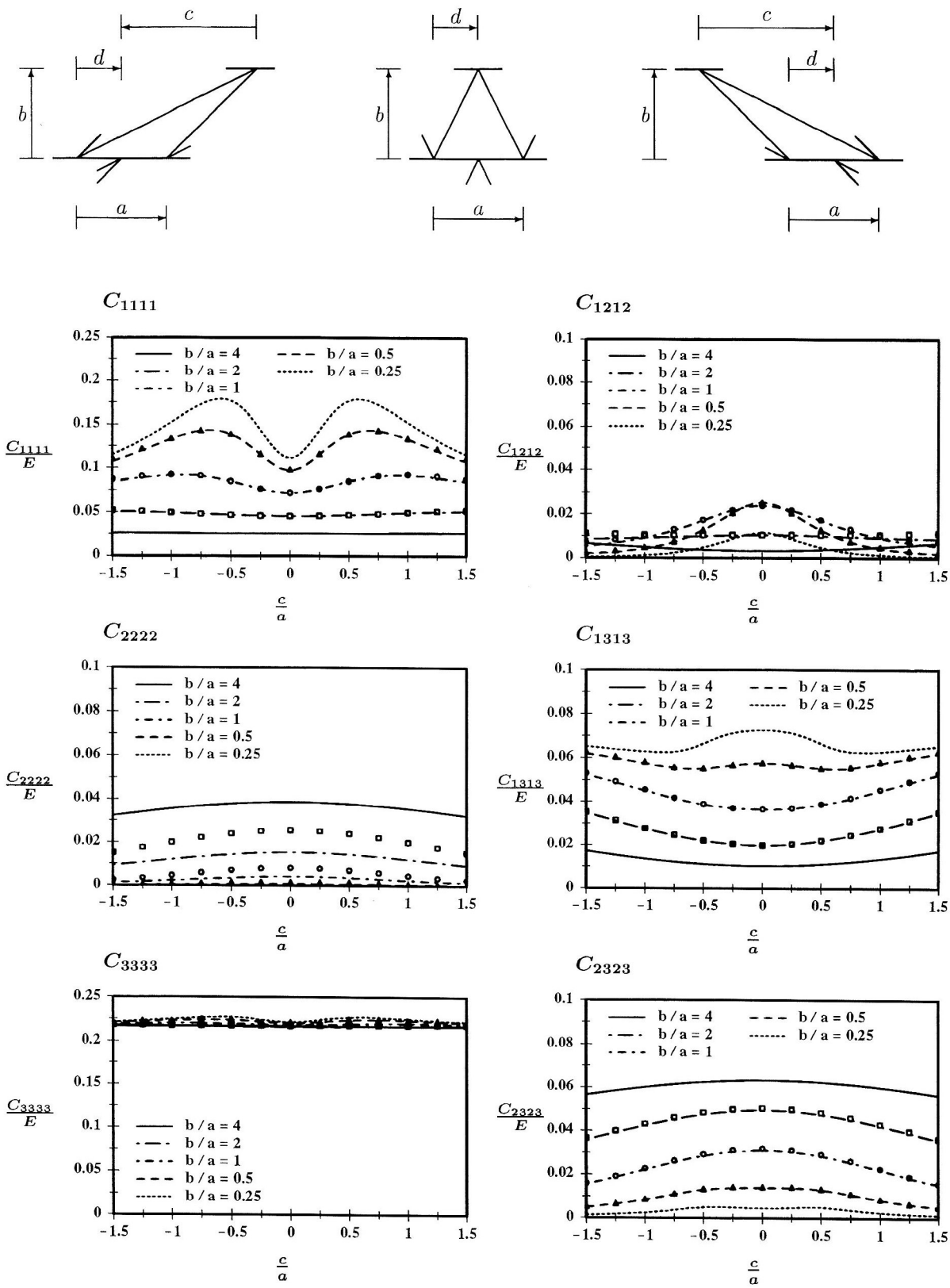

Figure 7: Effective Elastic Properties – Normal and Shear Components

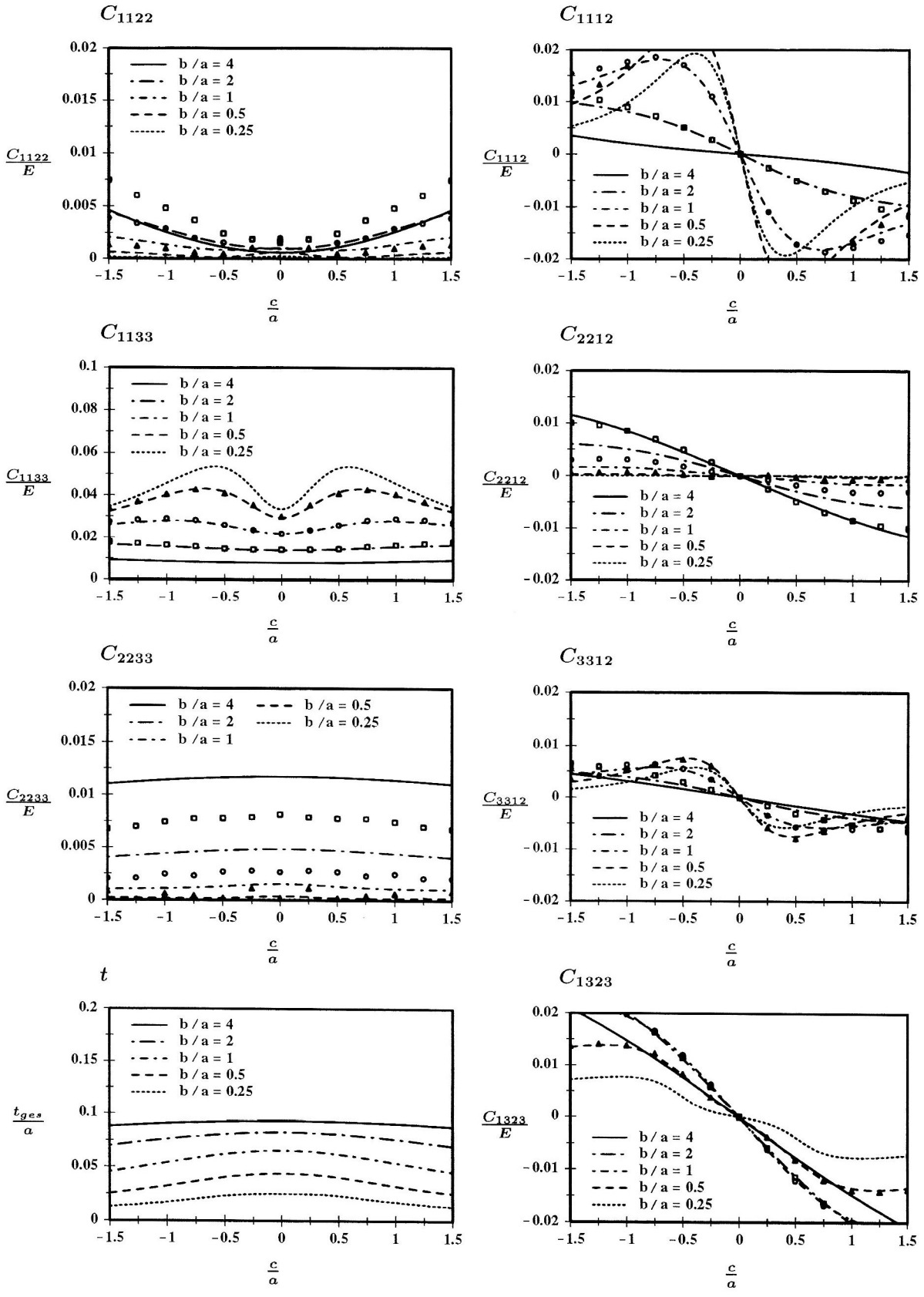

Figure 8: Effective Elastic Properties – Coupling Components

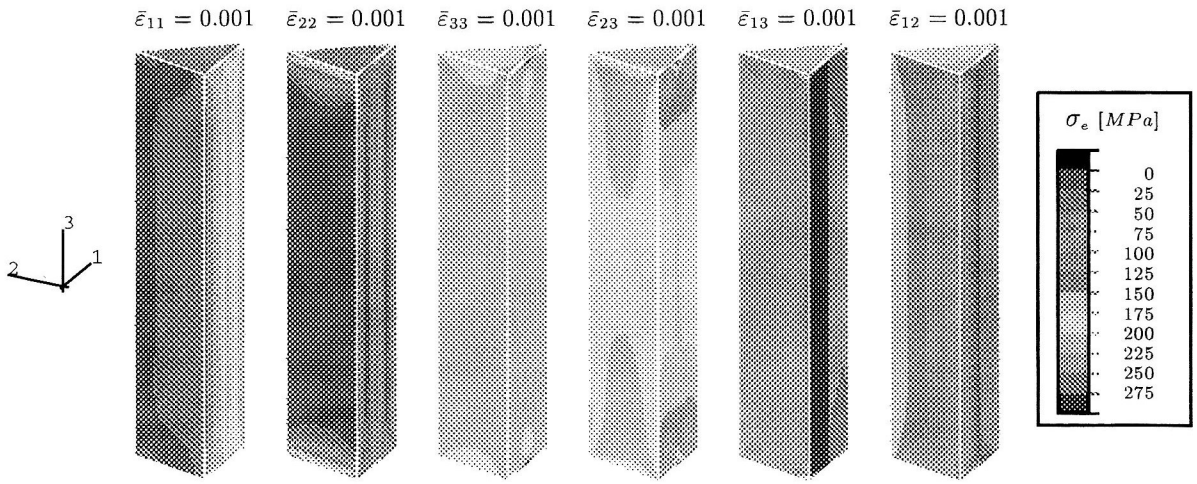

Figure 9: Distribution of v. Mises Equivalent Stress for Basic Modes of Deformation

In general, it can be observed that the normal and shear components increase, if an increasing number of cell walls is orientated with respect to the corresponding directions. Therefore, C_{2222} and C_{2323} attain their maximum, if $c/a \to 0$ since in this case, the inclined cell walls are in their most upright position. The opposite effect is observed in case of C_{1111} and C_{1313}. A partial decrease in the case of low b/a-values is caused by the decreasing cell wall thickness for decreasing b/a (see Figure 8). C_{3333} is strongly related to the relative density $\bar{\rho}$.

In case of the coupling components C_{1133} and C_{2233} (see Figure 8) a similar result as for the behaviour of the associated normal components C_{1111} and C_{2222}, respectively, is observed, which can be explained by the fact that C_{3333} is nearly constant. Since the triangular cell geometry under consideration is – in general – non-orthotropic, coupling of in-plane normal and shear deformation as well as coupling of the transverse shear deformation occurs. Therefore, the components C_{1112}, C_{2212}, C_{3312} and C_{1323} exist for all cases except $c/a = 0$ when orthotropic behaviour on the effective level is achieved.

Comparison of analytical and finite element results yields an excellent agreement except in the case of C_{2222} and the associated coupling components where a significant deviation is observed. This deviation is caused by the incompatibility of the deformation of the core and the face sheets. In load cases, where $\bar{\varepsilon}_{22}$ exists, the horizontal cell walls of the free cell structure (see Figure 6) are deformed in a bending mode while this line remains straight on the face sheets. Therefore, additional deformation of the cell walls occurs in the vicinity of the face sheets. This mode of deformation is incorporated into the finite element model but not into the analytical approach. In Figure 9, the distribution of the v. Mises equivalent stress from the finite element analysis for some basic load cases is presented. Here it is clearly observed that far from the face sheets a homogeneous distribution developes (as predicted by the analytical approach) while a significant increase occurs in some cases, as the face sheets are approached. Since this effect causes a dependence of the effective properties on the core thickness, it is often termed as thickness effect in literature (e.g. Becker, 1998).

6 Conclusion

In the present study, an effective material law for general twodimensional cellular materials has been developed. The material law is based on an energetic homogenization of the microstructure using the concept of the representative volume element. In this context, the strain energy stored in the representative volume element is evaluated comparatively by an analytical approach and by a pure numerical approach using the finite element method. Both approaches agree well except in cases, where strong core-face sheet constraints are present which are not incorporated in the analytical approach.

The advantage of the analytical method is that it enables the efficient computation of the effective properties of all kinds of cellular sandwich cores. Therefore it is useful especially for the design of optimized high-performance sandwich cores for special applications.

Acknowledgement

This work was financially supported by the Deutsche Forschungsgemeinschaft (DFG - german research association) under grant no. Be 1090/4-1.

Literature

1. Becker, W.: The inplane stiffness of a honeycomb core including the thickness effect. Arch. Appl. Mech., 68, (1998), 334-341
2. Bishop, J.F.W., Hill, R.: A theory of plastic distortion of a polycristalline aggregate under combined stress. Phil. Mag., 42, (1951), 414-427
3. Chang, C.C., Ebcioglu, I.K.: Effect of cell geometry on the shear modulus and on density of sandwich panel cores. J. Basic Eng., 83, (1961), 513-518
4. Gibson, L.J., Ashby, M.F.: Cellular solids. Pergamon Press, Oxford 1988
5. Hashin, Z., Shtrikman, S.: On some variational principles in anisotropic and nonhomogeneous elasticity. J. Mech. Phys. Solids, 10, (1962), 335-342
6. Hohe, J., Becker, W.: Effective elastic properties of triangular grid structures. Compos. Struct., (1999), to appear
7. Hohe, J., Beschorner, C., Becker, W.: Effective elastic properties of hexagonal and quadrilateral grid structures. Compos. Struct., (1999), to appear
8. Kelsey, S., Gellately, R.A., Clark, B.W.: The shear modulus of foil honeycomb cores. Aircraft Eng., 30, (1958), 294-302
9. Noor, A.K., Burton, W.S., Bert, C.W.: Computational models for sandwich panels and shells. Appl. Mech. Rev., 49, (1996), 155-199
10. Overaker, D.W., Cuitiño, A.M., Langrana, N.A.: Elastoplastic micromechanical modeling of two-dimensional irregular convex and nonconvex (re-entrant) hexagonal foams. J. Appl. Mech., 65, (1998), 748-757
11. Sanchez-Palencia, E.: Non-homogeneous media and vibration theory. Springer-Verlag, Berlin 1980
12. Torquato, S., Gibiansky, L.V., Silva, M.J., Gibson, L.J.: Effective mechanical and transport properties of cellular solids. Int. J. Mech. Sci., 40, (1998), 71-82

Address: Dr.-Ing. Jörg Hohe and Prof. Dr.-Ing. Wilfried Becker, Universität-GH Siegen, Institut für Mechanik und Regelungstechnik, Paul-Bonatz-Str. 9-11, D-57068 Siegen, Germany